Analytical solution for pressure driven viscid flow in ducts of different shape: application to human upper airways

B. Wu[a], A. Van Hirtum[a] and X. Luo[b]

[a]Gipsa-lab, UMR CNRS 5126, Grenoble Universities, 38000 Grenoble, France
[b]Department of Mathematics, University of Glasgow, G12 8QW Glasgow, UK
bo.wu@gipsa-lab.grenoble-inp.fr

Under the assumptions of incompressible, viscid, steady and parallel flow, analytical solutions are presented for fully developed pressure driven flow through uniform ducts with different cross section shapes. The considered geometries cover a wide range of shapes, which are relevant to different portions of the upper airways (e.g. glottis or/and oral tract) in normal or pathological conditions during breathing or speech production. In addition to the duct cross section shape, the cross section area in the main flow direction is varied in order to mimic upper airway portions in more detail. Besides the geometry, the Reynolds number is varied in a range relevant to the upper airways and speech production ($0 < Re < 10^4$). The effect of viscosity for the different geometries under study is discussed and comparision is based on either a fixed area or a fixed hydraulic diameter.

1 Introduction

Physical modelling of human speech production often relies on severe simplifications of the used mechanical, flow and acoustic models. The main reason for a simplified model approach relies in the limited number of remaining parameters which enables 1) experimental validation of physical models and 2) understanding of the influence of individual parameters. In this framework, the cross-section shapes encountered in the human upper airways are represented as either rectangular or circular whereas real life geometries vary considerable and more precise approximations can be used, such as an ellipse at the lips or as a triangle at the glottis during breathing. Therefore, in the current paper it is assessed to discuss the benefit of varying the cross section shape from circular or rectangular while maintaining the model approach commonly applied in physical modelling of human speech production and in particular phonation . Common flow models are derived from Bernoulli's one-dimensional flow equation corrected for viscous effects [1]. The current study will focus on the influence of the cross section shape on the viscous flow correction. Analytical solutions of viscous flow are favoured 1) in order to be integrated in existing models and 2) to be used as a validation for more complex flow models. Besides the velocity distribution important quantities for biomechanics such as the wall shear stress and associated friction factor can be derived. In the following sections, the different cross section shapes and channel geometries are introduced, the flow model is outlined and the model outcome is presented. A comparison between different cross section shapes is assessed by imposing either cross section area A or hydraulic diameter D.

2 Channel geometry

The channel geometry is fully defined by its shape (section 2.1) and the area along the main flow direction x (section 2.2). Main geometrical parameters are given in Table 2.

2.1 Uniform channel: cross section shape

In order to allow the use of the cross section shapes in quasi analytical models only cross sections shapes for which the main geometrical parameters can be expressed analytically are assessed (Fig. 1): rectangle (re), circle (cl), ellipse (el), eccentric annulus (ea), half moon (hm), circular section (cs), equilateral triangle (tr) and limacon (lm). The cross section is positioned in the (y, z) plane where y denotes the spanwise and z the transverse direction. An analytical expression of the shape can be obtained in terms of the parameters a and b. A uniform channel is fully defined by its cross section shape and its cross section area A. An important additional

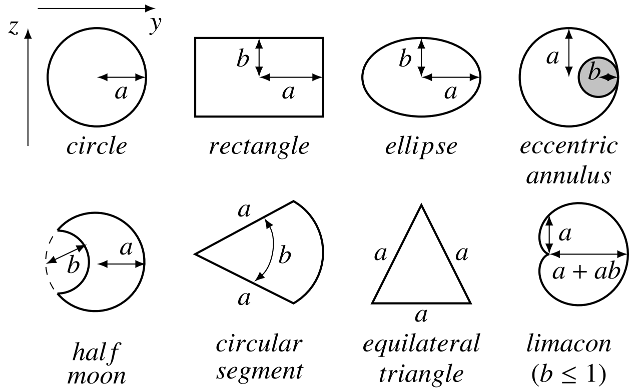

Figure 1: Different cross section shapes in the (y, z) plane.

parameter is the ratio of area to perimeter S or hydraulic diameter $D = 4A/S$ given in Table 1.

Table 1: Hydraulic diameter D for which the subscript indicates the cross section shape. Geometrical parameters are given between straight brackets.

Cross section shape	Hydraulic diameter D
circle $[a]$	$D_{cl} = 2a$
ellipse $[a, b]$	$D_{el} = \frac{4ab}{a+b}\left(\frac{64-16c^2}{64-3c^4}\right)$ $c = \frac{a-b}{a+b}$
rectangle $[a, b]$	$D_{re} = \frac{4ab}{a+b}$
equilateral triangle $[a]$	$D_{tr} = \frac{a}{\sqrt{3}}$
circular[1] segment $[a, b]$	$D_{cs} = \frac{2ab}{2+b}$
eccentric annulus $[a, b]$	$D_{ea} = 2(a - b)$
half moon $[a, b]$	$D_{hm} = \frac{4A_{hm}}{(\pi-\theta_2)(2a+b)}$ $A_{hm} = a^2\left(\pi - \theta_2 + \frac{1}{2}\sin(2\theta_2)\right)$ $-\frac{b^2}{2}(\pi - \theta_2 - \sin(\theta_2))$ $\theta_2 = 2\arcsin(\frac{b}{2a})$
limacon $[a, b]$ (polar form $r(\theta)$)	$D_{lm} = 2a(2 - 4/(b^2 + 4))$ $b \leq 1, a = r(\theta = \pi/2)$

[1] b indicates an angle instead of a length (see Fig. 1).

2.2 Converging-diverging channel

A channel with varying cross section area in the longitudinal x direction and fixed shape is of interest. It is sought to vary the parameter $f(x)$ describing the cross section, *i.e.* concretely $f(x)$ denotes either area $A(x)$ or hydraulic diameter $D(x)$, in a prescribed manner. $f(x)$ is obtained following a combination of control parameters (Fig. 2(a)): maximum value f_0, minimum value $f_{min} < f_0$, total channel length L, constriction length L_c and a prescribed transition function describing the transition from f_0 to f_{min} upstream and downstream from the constriction. Besides a sine function (illus-

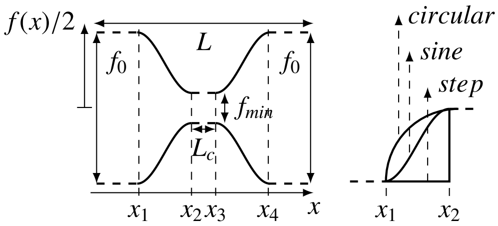

(a) varying $f(x)$ (b) transition

Figure 2: a) varying $f(x)$: sine transition function, constriction length L_c, minimum f_{min}, maximum f_0 and total channel length L. b) transition functions for $x_1 \leq x \leq x_2$.

trated in Fig. 2(a)) several transition functions can be used to prescribe the diverging or converging portion of the transition from f_0 to f_{min}, *i.e.* upstream and/or downstream from the constriction in the intervals $I_1 = [x_1 \ x_2]$ and $I_2 = [x_3 \ x_4]$, respectively. Concretely, a sine, step or circulary rounded transtion is used to describe the transition for $x \in I_{1,2}$ as depicted in Fig. 2(b).

Table 2: Overview of main geometrical parameters.

Cross section	Channel geometry	
	Uniform	Converging-diverging
shape a, b	√	√
hydraulic[1] diameter D	√	√
maximum f_0	√	√
transition $f(x_1 \leq x \leq x_2)$	-	√
transition $f(x_3 \leq x \leq x_4)$	-	√
minimum f_{min}, L_c	-	√

[1] or area $A = \pi \frac{D_{cl}^2}{4}$.

3 Viscous flow model

The flow model and its underlying assumptions are outlined for pressure driven viscous flow through a channel. Using the parameters summarised in Table 2 flow through a uniform (section 3.1) as well as converging-diverging (section 3.2) channel needs to be modelled.

3.1 Uniform channel

For a given fluid and under the assumptions of a laminar, incompressible, parallel and steady viscous flow through a uniform channel with arbitrary but constant shape, such as the cross sections discussed in section 2.1, the streamwise component of the momentum equation expressed in cartesian coordinates (x, y, z) reduces to the following Poisson equation:

$$\frac{\partial^2 u}{\partial y^2} + \frac{\partial^2 u}{\partial z^2} = \frac{1}{\mu}\frac{dP}{dx}, \qquad (1)$$

the spanwise and transverse components of the momentum equation become:

$$\frac{\partial P}{\partial y} = 0, \ \frac{\partial P}{\partial z} = 0 \qquad (2)$$

and the continuity equation yields:

$$\frac{\partial u}{\partial x} = 0, \qquad (3)$$

describing fully developed flow in the streamwise x direction, driving pressure difference dP/dx, velocity $u(x, y, z)$ and fluid properties, *i.e.* dynamic viscosity μ, density ρ and their ratio which yields kinematic viscosity $\nu = \mu/\rho$. A no slip condition on the boundaries is imposed so that $u = 0$ on the channel walls. The driving pressure difference is defined as

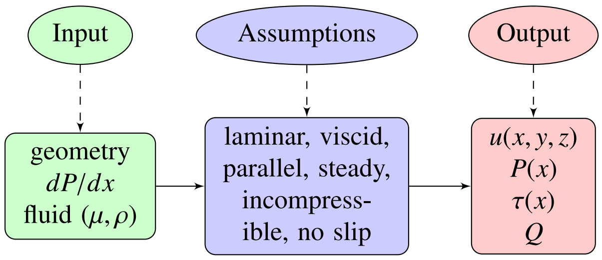

Figure 3: Overview of pressure driven viscous flow model.

the difference between the upstream pressure $P_{up} = P_0$ and downstream pressure $P_d = 0$ so that $dP/dx = P_0$ holds. For air, the fluid properties yield $\mu = 1.8 \times 10^{-5}$ Pa/s, $\rho = 1.2$ kg/m^3 and $\nu = 1.5 \times 10^{-5}$ m^2/s. For uniform geometries and applying the no slip boundary condition Eq. 1 can be rewritten as a classical Dirichlet problem which can be solved analytically for simple geometries using *e.g.* separation of variables since both sides of Eq. 1 are constant. Therefore exact solutions can be obtained for: local velocity $u(x, y, z)$, local pressure $P(x)$, wall shear stress $\tau(x)$ and derived quantities such as volume flow rate Q. Underlying flow assumptions, model input and model output quantities are summarised in Fig. 3. As an example, analytical solutions for the cross section shapes depicted in Fig. 1 are given in Table 3 for the volume flow rate Q as function of the driving pressure difference dP/dx. Note that the parameters a and b vary with the cross section shape as shown in Fig. 1. Once the volume flow rate Q is known the bulk Reynolds number Re is estimated as $Re = \frac{QD}{\nu A} = \frac{u_b D}{\nu}$, where u_b denotes the bulk velocity $u_b = Q/A$. Although the model is pressure driven as depicted in Fig. 3, the model output Q (or Re or u_b) can be used to control the model instead of the driving pressure dP/dx by using a relaxation method or by using an analytical relationship between $Q(dP/dx)$ as given in Table 3.

3.2 Converging-diverging channel

A non uniform channel with constant cross section shape is obtained by introducing a streamwise converging-diverging portion in an otherwise uniform channel by prescribing a geometrical parameter $f(x)$, *i.e.* either area A or hydraulic diameter D, as outlined in section 2.2. Application of the transition functions, to describe the transition from the uniform channel portion characterised by f_0 to the minimum value f_{min}, results in a channel geometry which is characterised by

Table 3: Illustration of analytical solutions. Geometrical parameters a and b are as depicted in Fig. 1.

Cross section	Volume flow rate $Q\left(\frac{dP}{dx}\right)$
circle	$\frac{\pi a^4}{8\mu}\left(-\frac{dP}{dx}\right)$
ellipse	$\frac{\pi}{4\mu}\left(-\frac{dP}{dx}\right)\frac{a^3b^3}{a^2+b^2}$
rectangle[1]	$\frac{4a^3}{3\mu}\left(-\frac{dP}{dx}\right)\left[b-\frac{192\alpha}{\pi^5}\sum_{n=1,3,\ldots}^{\infty}\frac{\tanh(n\pi b/2a)}{n^5}\right]$
equilateral triangle	$\frac{\sqrt{3}a^4}{320\mu}\left(-\frac{dP}{dx}\right)$
circular segment[1]	$\frac{a^4}{4\mu}\left(-\frac{dP}{dx}\right)[\frac{\tan b-b}{4}-$ $\frac{32b^4}{\pi^5}\sum_{n=1,3\ldots}^{\infty}\frac{1}{n^2(n+2b/\pi)(n+b/\pi)(n-2b/\pi)}]$
eccentric annulus[1,2]	$\frac{\pi}{8\mu}\left(-\frac{dP}{dx}\right)\left[a^4-b^4-\frac{4c^2M^2}{\beta-\alpha}-\right.$ $\left.8c^2M^2\sum_{n=1}^{\infty}\frac{ne^{-n(\beta+\alpha)}}{\sinh(n\beta-n\alpha)}\right]$ $0<c\leq a-b,\ F=\frac{a^2-b^2+c^2}{2c}$ $M=\sqrt{(F^2-a^2)}$ $\alpha=\frac{1}{2}\ln\frac{F+M}{F-M},\ \beta=\frac{1}{2}\ln\frac{F-c+M}{F-c-M}$
half moon	$\frac{1}{4\mu}\left(-\frac{dP}{dx}\right)\left[(2a^3b+\frac{21}{12}ab^3)\sin(\theta_1)+\right.$ $\left.(a^4-\frac{b^4}{2}-2a^2b^2)\theta_1\right]$ $\theta_1=\arccos(b/2a)$
limacon	$\frac{\pi}{8\mu}\left(-\frac{dP}{dx}\right)a^4\left(1+4b^2-2b^4\right)$

[1] infinite sum is limited to $n \leq 60$.

[2] c yields the distance between inner and outer circle centers.

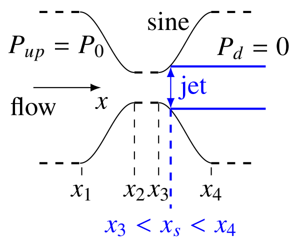

(a) smooth expansion (sine)

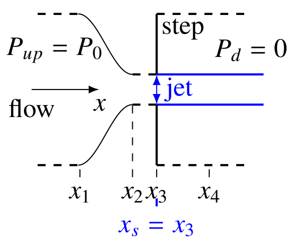

(b) abrupt expansion (step)

Figure 4: Illustration of flow through a converging-diverging channel: a) smooth expansion, b) abrupt expansion.

a smooth or abrupt expansion as schematically illustrated in Fig. 4. The main effects of a converging-diverging channel portion on the flow are an important flow acceleration in the constricted portion and the occurrence of jet formation associated with flow separation due to flow retardation along the divergent portion. In case of an abrupt expansion characterised by a sharp trailing edge, the streamwise position of flow separation x_s is fixed at the constriction end, so that $x_s = x_3$ as in Fig. 4(b). In case of a smooth expansion, the flow separation position depends on the channel geometry as well as on the imposed driving pressure dP/dx, so that $x_3 \leq x_s \leq x_4$ as in Fig. 4(a). The simplest way to model the moving separation position is to assume that at the separation position $x = x_s$ the transition function yields $f(x_s) = c \times f_{min}$ where the constant c is set to $c = 1.2$ in accordance with literature [1]. The pressure downstream from the flow separation point is assumed to be constant and zero so that $P_d = 0$ holds for $x \geq x_s$ and the model outcome remains constant for $x \geq x_s$. Consequently, as before, imposing the upstream pressure $P_{up} = P_0$ allows to impose the driving pressure difference $dP/dx = P_0$. The flow in the converging section undergoes a strong streamwise acceleration due to the Bernoulli effect which is not accounted for in case of a purely viscous flow model (Eq. 3). Nevertheless, depending on driving pressure and geometry, in particular f_{min} and L_c, the contribution of viscous effects to the flow becomes important or even dominant compared to flow inertia effects.

4 Results

The influence of geometrical and flow parameters on the model outcome is assessed for a uniform channel (section 4.1) and a converging-diverging channel (section 4.2). The model input parameters are extensively varied in a range relevant to flow through the human upper airways. A comparison between different cross section shapes is assessed by prescribing either cross section area A or hydraulic diameter D, corresponding to setting either $f(x) = A(x)$ or $f(x) = D(x)$, as outlined in section 2. The circle cross section shape as well as the shape of an equilateral triangle are fully described by one parameter a whose value follows directly from the imposed A or D. For the remaining cross section shapes, an additional condition is necessary to obtain the geometrical parameter set $[a\ b]$ illustrated in Fig. 1. Unless stated differently, the following conditions (default) are applied: $a_{re} = 1a_{cl}$, $a_{el} = 1.2a_{cl}$, $b_{ea} = 0.2a_{ea}$, $b_{cs} = \pi/3$, $b_{hm} = 0.3a_{hm}$ and $b_{lm} = 1$. Resulting $D(A)$ and $A(D)$ are illustrated in Fig. 5 as well as the total spanwise length $y_{tot}(A)$ and total transverse length $z_{tot}(A)$. Shown values are normalised with respect to the circle. The resulting $A(D)$ and $D(A)$ vary between values

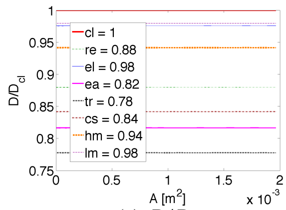

(a) D/D_{cl}

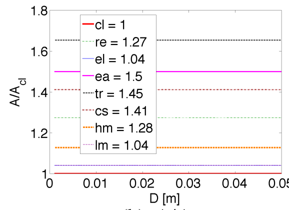

(b) A/A_{cl}

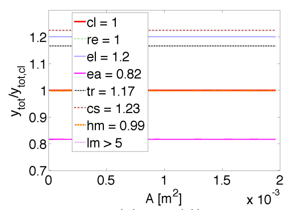

(c) $y_{tot}(A)$

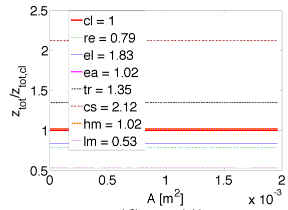

(d) $z_{tot}(A)$

Figure 5: a) imposing area: $D(A)$, b) imposing hydraulic diameter: $A(D)$, c) total spanwise length $y_{tot}(A)$ and d) total transverse length $z_{tot}(A)$.

obtained for a circle and an equilateral triangle: with 65% for $A(D)$ and with 32% for $D(A)$. The variation of the total transverse length is more pronounced than the variation of the transverse length do to the imposed additional condition. The total transverse and spanwise lengths of the limacon does not follow the same tendencies as observed for the other assessed cross sections. So that no constant value for $y_{tot}/y_{tot,cl}$ is obtained in case of a limacon.

4.1 Uniform channel: cross section shape

The influence of the cross section shapes, depicted in Fig. 1, on the model outcome is assessed. Fig. 6 illustrates the velocity distribution $u(y/a_{cl}, z/a_{cl})$ for a fixed area A and dP/dx. The maximum velocity varies between 9 m/s for

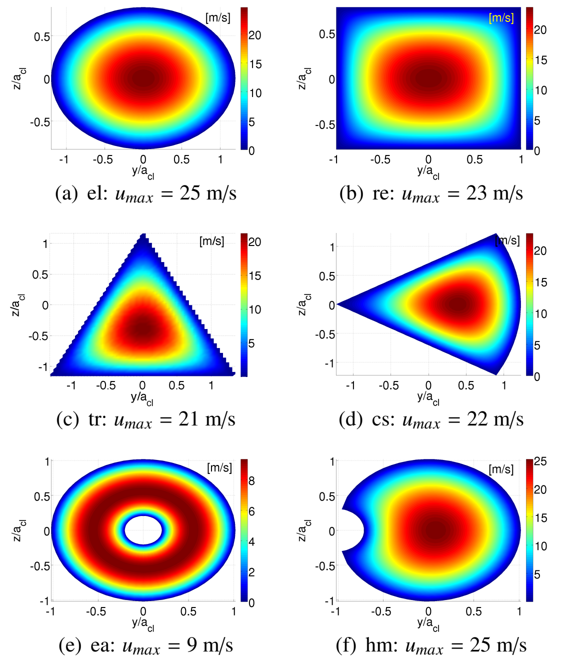

(a) el: u_{max} = 25 m/s (b) re: u_{max} = 23 m/s

(c) tr: u_{max} = 21 m/s (d) cs: u_{max} = 22 m/s

(e) ea: u_{max} = 9 m/s (f) hm: u_{max} = 25 m/s

Figure 6: $u(y/a_{cl}, z/a_{cl})$ for $A = 79$ mm^2 and $dP/dx = 75$ Pa. For a circle, $u_{max} = 26$ m/s holds.

a concentric annulus and 40 m/s for the circular segment. The velocity distribution is seen to preserve spatial symmetry. Note that the equilateral triangle is not symmetric for $z = 0$ since the maximum velocity yields $z/a_{cl} \simeq -0.4$, *i.e.* $z/a_{cl} = a_{tr}/a_{cl} \cdot \left(\sqrt{(3)}/6 - 1\right)/2$, whereas for the circular section symmetry is maintained. Since for the shown geometrical configuration the angles are set to $\pi/3$ in both cases, it is seen that varying the base from straigth to circular allows to perturb the position of symmetry, which is likely a realistic perturbation configuration. Normalised spanwise velocity profiles containing the maximum velocity are illustrated in Fig. 7. Most profiles - circular, elliptic, triangular

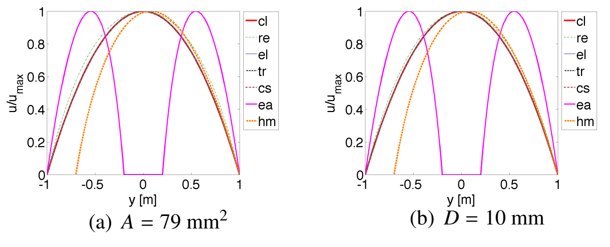

(a) $A = 79$ mm^2 (b) $D = 10$ mm

Figure 7: Normalised spanwise velocity profile for $dP/dx = 75$ Pa: a) A imposed, b) D imposed.

and circular segment - collapse to a single curve. The rectangular section profile is broader than for the circle and obviously the concentric annulus profile presents two maxima. The maximum of the half moon profile is shifted to $y > 0$. The maximum velocity normalised with respect to the maximum velocity of a circular cross section with the same area A or with the same hydraulic diameter D as function of the imposed pressure difference dP/dx is shown in Fig. 8(a) and Fig. 8(b). The corresponding normalised values of the volume flow rate are shown in Fig. 8(c) and Fig. 8(d). The values of the imposed quantities A and D are not indicated since the

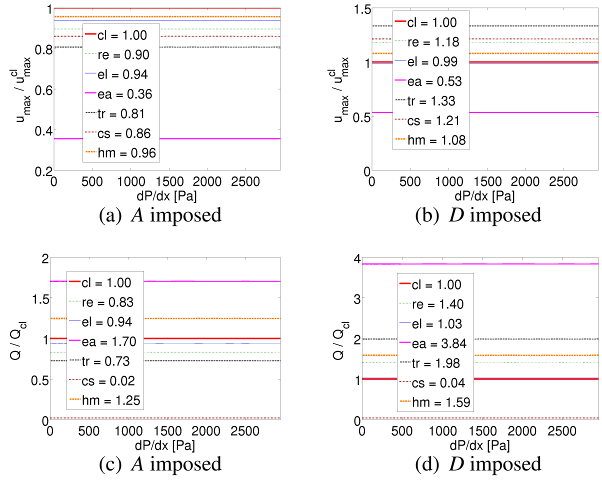

(a) A imposed (b) D imposed

(c) A imposed (d) D imposed

Figure 8: Normalised $u_{max}(dP/dx)$ and $Q(dP/dx)$: a,c) A imposed and b,d) D imposed.

normalised values of u_{max}/u^{cl}_{max} and Q/Q_{cl} are independent from the imposed dP/dx, as illustrated by the constant value in the figure and legend, as well as from the imposed area A or from the imposed hydraulic diameter D. Consequently, the values of u_{max}/u^{cl}_{max} and Q/Q_{cl} depend only on the cross section shape. For Q/Q_{cl} this is also observed from Table 3. The normalised mean wall shear stress, shown in Fig. 9, is dependent on the cross section shape as well as on the value of the imposed area A or hydraulic diameter D and on the imposed pressure difference dP/dx since its value increases as dP/dx decreases and as the imposed A or D decreases. The influence of varying the cross section shape parameters

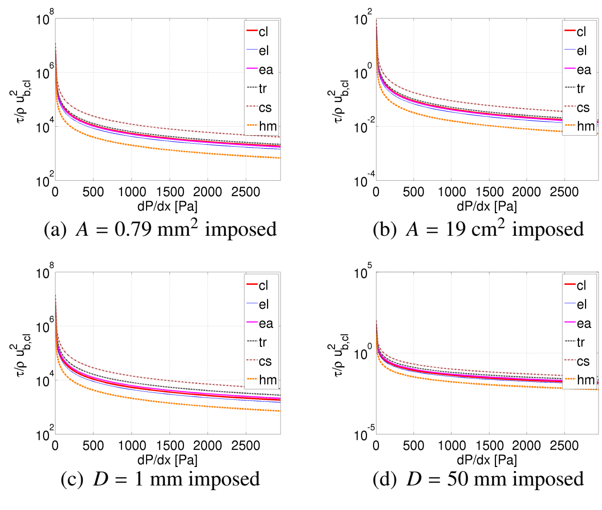

(a) $A = 0.79$ mm^2 imposed (b) $A = 19$ cm^2 imposed

(c) $D = 1$ mm imposed (d) $D = 50$ mm imposed

Figure 9: $\tau(dP/dx)$: a,b) A imposed and c,d) D imposed.

from their default values (labelled α_0) is assessed by varying α ($a_{re} = \alpha_{re} a_{cl}$, $a_{el} = \alpha_{el} a_{cl}$, $b_{ea} = \alpha_{ea} a_{ea}$, $b_{cs} = \alpha_{cs}$, $b_{hm} = \alpha_{hm} a_{hm}$ and $b_{lm} = \alpha_{lm}$) as shown in Fig. 10. Results are obtained for a constant area A and pressure difference dP/dx. Except for a circular segment (cs), it is seen that the effect of viscosity increases with α. For a rectangular ($\alpha_{re} \geq \sqrt{\pi/4}$, deviation from a square) and elliptic cross section ($\alpha_{cl} \geq 1$, deviation from a circle) increasing $\alpha_{re,cl} \gtrsim 10$ does not influence the effect of viscosity. In case of a circular segment, increasing the angle of the segment decreases the influence of viscosity at first until $\alpha_{cs} \simeq 85^o$. Further increasing the angle enforces the influence of viscosity, so that the ratio u_{max}/u^{cl}_{max}

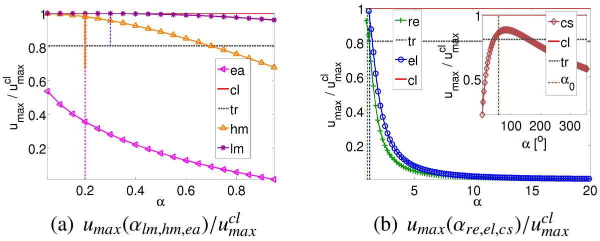

(a) $u_{max}(\alpha_{lm,hm,ea})/u^{cl}_{max}$ (b) $u_{max}(\alpha_{re,el,cs})/u^{cl}_{max}$

Figure 10: Influence of geometrical parameter α on u_{max}/u^{cl}_{max}. Vertical lines indicate default values (α_0).

decreases and finally approximates the value associated with a concentric annulus for which the smallest internal radius corresponds to $\alpha_{ea} = 0.05$.

4.2 Converging-diverging channel

The pressure drop obtained from a quasi one dimensional flow in a two dimensional converging-diverging channel with fixed width is illustrated in Fig. 11 [1] for varying transition function, constriction length L_c and upstream pressure P_0. The area $A(x)$ is imposed at each streamwise position. The convergent portion of the geometry introduces a pres-

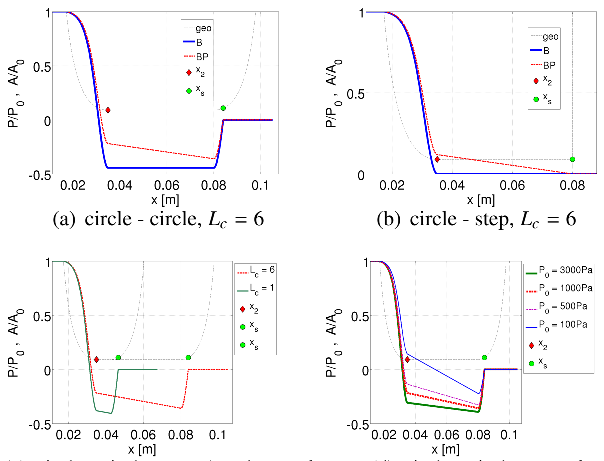

(a) circle - circle, $L_c = 6$ (b) circle - step, $L_c = 6$ (c) circle - circle, $L_c = 1$ and $L_c = 6$ (d) circle - circle, $L_c = 6$

Figure 11: Quasi one dimensional normalised pressure $P(x)/P_0$ (ideal fluid (B) with viscous correction(BP)) for $f_{min}/f_0 = 0.3$ and imposing $A(x)$: a,b) varying upstream and downstream transition functions for $P_0 = 1000$Pa, c) varying constriction length ($L_c = 1$ and $L_c = 6$) for $P_0 = 1000$Pa and d) varying upstream pressure P_0.

sure drop along the constricted portion due to the Bernoulli effect. Accounting for viscosity (and assuming that the channel width equals to the unconstricted channel height f_0) within the constriction severly alters the pressure distribution since the viscous term is the only flow actor downstream from the onset of the uniform constricted portion up to the flow separation point. Fig. 11(c) illustrates that prolonging the constricted region reduces the pressure drop due to the convergent portion until that eventually the pressure remains positive as is observed in case of a downstream step transition in Fig. 11(b). Varying the continuous transition function influences the pressure distribution to a less extent and is therefore not shown in Fig. 11. The viscous contribution to the pressure drop decreases as the upstream pressure increases, as shown in Fig. 11(d), whereas the convection portion remains constant for a constant geometry. In Fig. 11 the viscous contribution is accounted for using a quasi one dimensional correction. Fig. 12 illustrates the pressure distribution in case the cross section shape is accounted for. Default and non default geometrical conditions α are applied:

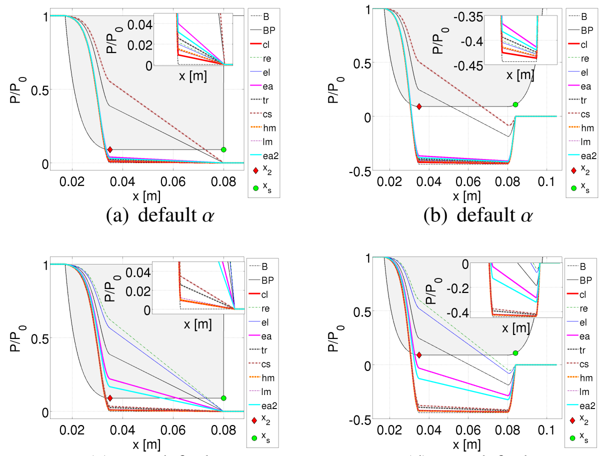

(a) default α (b) default α (c) non default α (d) non default α

Figure 12: Normalised pressure $P(x)/P_0$ for $f_{min}/f_0 = 0.3$, $L_c = 6$, $P_0 = 1000$ and imposing $A(x)$ for ideal fluid (B), ideal fluid with quasi one dimensional viscous correction (BP) and viscous flow as function of α: a,c) upstream circle and downstream step transition and b,d) upstream and downstream circle transition. Label 'ea' and 'ea2' indicate a concentric and eccentric annulus.

$a_{re} = 5a_{cl}$, $a_{el} = 5a_{cl}$, $b_{ea} = 0.6a_{ea}$, $b_{cs} = \pi/6$, $b_{hm} = 0.6a_{hm}$ and $b_{lm} = 0.6$. Note that α_{cl} and α_{tr} follow directly from the imposed area $A(x)$. Non default geometrical conditions are chosen so that for a uniform geometry (Fig. 10) the viscous contribution is altered. For default α values (Fig. 12(a) and Fig. 12(b)) the viscous contribution to the pressure drop for all cross sections, except the circular section, is low. Therefore, the pressure drop is close to the value obtained from the Bernoulli term neglecting viscosity. The quasi one dimensional viscous contribution overestimates ($\geq 20\%$) the pressure loss within the constricted portion. For non default α values (Fig. 12(c) and Fig. 12(d)) the pressure drop varies from near the value of no viscosity (triangle or half moon) to well above (10% or more) the quasi one dimensional viscous contribution, as *e.g.* observed for a rectangular or elliptic cross section.

5 Conclusion

The influence of the cross section shape on viscous flow development in a uniform and convergent-divergent channel is assessed. The relevance for a quasi one dimensional approximation of the viscous term can be questioned for conditions favoring boundary layer development.

References

[1] J. Cisonni, A. Van Hirtum, X. Pelorson, and J. Willems. Theoretical simulation and experimental validation of inverse quasi one-dimensional steady and unsteady glottal flow models. *J. Acoust. Soc. Am.*, 124:535–545, 2008.